Fabrication and Performance of a Spherical Cellulose Nanocrystal-based Hydrophobic Drug Delivery Vehicle using Rubber Wood

Dingyuan Zheng, Yating Deng, Yue Xia, Yiman Nan, Meijiao Peng, Xinduo Wang, and Jinque Yue *

Cellulose nanocrystals (CNCs) were fabricated using rubber wood (RW) as the raw material *via* acid hydrolysis followed by ultrasonication. The CNCs samples were then grafted with succinic anhydride to obtain modified CNCs, hereafter called CS. The CS samples were subsequently coated with a cationic surfactant, cetyltrimethyl ammonium bromide, and the obtained samples were named as CC. The morphology, chemical structure, and thermal stability of the RW, CNCs, CS, and CC samples were characterized using transmission electron microscopy, Fourier-transform infrared spectroscopy, and thermogravimetric analysis, respectively. Finally, the drug release performance was investigated using CC as the drug carrier and hesperidin, a hydrophobic drug, as the model drug. The drug release mechanism was also considered. The results of this study identified a new route for the high-value utilization of RW and also demonstrated that RW could be used as a novel substrate for the construction of cellulose-based hydrophobic drug delivery systems.

Keywords: Drug delivery vehicle; Cellulose nanocrystals; Rubber wood; Hesperidin

Contact information: Key Laboratory of Bio-based Material Science and Technology of Ministry of Education, College of Material Science and Engineering, Northeast Forestry University, Harbin 150040, R P China;
** Corresponding author: yuejinq@163.com*

INTRODUCTION

Hesperidin (HES), molecular formula $C_{28}H_{34}O_{15}$, relative molecular weight 610.55, is the predominant polyphenol consumed from citrus fruits and juices (Nielsen *et al*. 2006). It has been reported that hesperidin provides benefits including anti-oxidation, anti-cancer, anti-inflammatory, bacteriostasis, and improvement of the central nervous system. Although this compound has great medicinal potentiality, poor water solubility (1g/50 L, HES/water) limits its application (Tripoli *et al*. 2007). In order to overcome the issue, potential drug delivery vehicles need to be fabricated urgently.

Cellulose nanocrystals (CNCs) are rodlike-shaped crystalline cellulose particles that are obtained by removing the disordered regions in native cellulose microfibrils (Boluk *et al*. 2011). CNCs have been isolated from a wide variety of cellulosic resources, including wood (Sacui *et al*. 2014), bamboo (Brito *et al*. 2012), sisal (Mondragon *et al*. 2018), and sugarcane bagasse (Camargo *et al*. 2016). CNCs are environmentally friendly and are considered as having potential value due to their low density (1.6 g-cm^{-3}), high elastic modulus (130 GPa), high crystallinity, low toxicity, biodegradability, and simple chemical modification (Habibi *et al*. 2010). Furthermore, the CNCs surface has a large number of -OH groups, and it can be used as a functional template carrier for multifunctional design and compounding, due to its high surface area and high aspect ratio (Beck-Candanedo *et al*. 2005). It has been reported that CNCs, which help in regulating swelling behavior of hydrophilic polymers *via* various types of interactions

such as covalent bonds, hydrophilic bond, and hydrophobic interactions, could be utilized as nanofillers to control drug release (Hasan *et al*. 2017, 2018). Additionally, CNCs possess good biocompatibility (Rao *et al*. 2017). Therefore, CNCs and their derivatives have received extensive attention in the fields of biological materials and drug delivery (Kontturi *et al*. 2018), with broad prospects in the preparation of cellulose-based drug delivery systems.

Rubber wood (RW) is a fast-growing tree that is primarily used to provide cut rubber and is cultivated on numerous tree plantations in southern China. More than 2 million cubic meters of rubber logs are currently produced annually in China, which has become one of the most important sources of the Chinese wood supply, as well as an important species for sustainable recycling (Qin *et al*. 2017). Rubber trees are widely used in furniture manufacturing once their ability to produce rubber diminishes (Li *et al*. 2016). However, much of the RW is still used as fuel (Huang 2008), despite its low utilization value, making it a serious environmental pollutant. It has been reported that RW contains approximately 50% cellulose (Zheng *et al*. 2019), making it a potentially significant raw material for CNCs. RW-based CNCs fabrication could provide a new route for the high-value utilization of RW while also mitigating the environmental pressure posed by extensive RW burning.

In this work, CNCs were prepared from RW *via* sulfuric acid hydrolysis, in combination with high-intensity ultrasonication, to better assess their application prospects as a drug carrier. Torispherical CNCs were prepared, since they are more suitable for drug delivery systems due to their large surface area compared to rod like-shaped CNCs. Succinic anhydride (SAA) was utilized to introduce carboxylic groups, which could provide more negative charges on the CNCs *via* a ring-opening esterification reaction (Sehaqui *et al*. 2017), with the modified CNCs, hereafter called CS. The hydrophobicity of CS was increased *via* coating with cetyltrimethyl ammonium bromide (CTMAB), a cationic surfactant (Wu *et al*. 2011), due to the anionic groups (sulfate, hydroxyl, and carboxyl groups) on the CS surface. The coated CS will be referred to as CC for the rest of this paper. Herein, the morphology and structure of RW, CNCs, CS, and CC were characterized *via* F-SEM, TEM, and FTIR. All samples were characterized by TGA to determine the effect of modification on the thermal stability of samples. Finally, the CC was used as drug delivery vehicle and then the drug release performance of hesperidin (HES) from CC@HES was studied to assess the fabricated drug delivery system. This work would offer novel routes for high-valued utilization of RW and provide new biomass materials for the construction of drug delivery systems.

EXPERIMENTAL

Materials

RW was obtained from Dan Zhou, Hainan Province, China. All of the chemicals were of analytical grade and supplied by Tianjin Kemiou Chemical Reagent Co., Ltd. (Tianjin, China). SAA and HES were purchased from Aladdin Reagent Co., Ltd. (Shanghai, China). The water used in the experiments was double distilled water.

Preparation and Modification of the CNCs

RW was pretreated according to previous studies to remove hemicelluloses, lignin, protein, and starch (de Rodriguez *et al*. 2006). RW was pulverized into smaller units and sieved using a 60-mesh (0.25 mm). The powder was then washed four times in a boiling 2 wt% aqueous NaOH solution for 4 h and mechanically stirred, with the powder filtered and rinsed using double distilled water between each treatment step. There was no significant discoloration of the NaOH

solution during the last treatment. A subsequent bleaching treatment at 80 °C for 6 h was used to render the powder white. The bleaching solution contained equal parts of aqueous chlorite (1.7 wt% $NaClO_2$ in water) and an acetate buffer (27 g of NaOH and 75 mL of glacial acetic acid, which was diluted to 1 L using double distilled water). The powder content was approximately 5 wt%, and the bleaching step was repeated three times, with the powder filtered and rinsed using double distilled water between each treatment step. The obtained purified cellulose fibers were subsequently dried at 40 °C for 24 h in a convection oven.

The CNCs suspension was prepared *via* sulfuric acid hydrolysis (Brito *et al*. 2012) of the purified cellulose fibers. The purified cellulose fibers (10 g) were first treated with 87.5 mL of a sulfuric acid solution (64 wt%) at 45 °C for 1 h under constant magnetic stirring (600 rpm). The reaction was terminated by adding 1 L of double distilled water, and the suspension was subsequently washed four to five times by successive centrifugation at 12000 rpm until a turbid supernatant became visible. The suspension was dialyzed until the water had a pH of 6 to 7. The suspension was then transferred and treated with high-intensity ultrasonication at 600 W for 30 min to obtain spherical CNCs (Qing *et al*. 2016). The CNCs were then collected *via* freeze-drying.

SAA was grafted onto the CNCs hydroxyl groups to synthesize CS as follows. CNCs (1.0 g) was dispersed in 50 mL of dimethylacetamide and 1 mL of pyridine with constant magnetic stirring (800 rpm, 40 min). This was followed by the addition of SAA (6.2 g) to the mixture in an oil bath (100 °C, 10 h). The obtained products were repeatedly filtered and washed with chloroform to remove any unreacted monomers. The fabricated CS powder was then collected *via* freeze-drying.

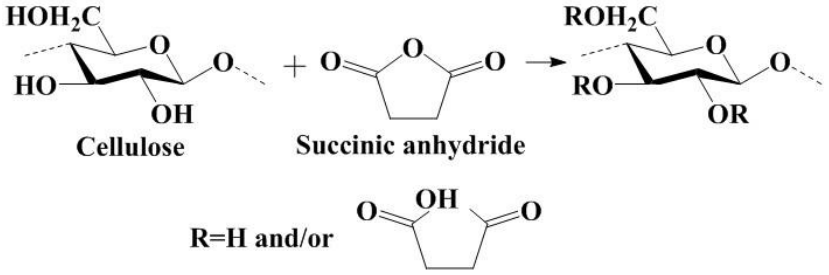

Fig. 1. Modification of CNC with SAA

Preparation of the Drug Carrier (CC)

The reaction was performed according to Qing *et al*. 2016. The CS (0.05 g) and 25 mL of the CTMAB solution (0.8 g L^{-1}) were added to a reactor. The mixture was stirred at 500 rpm and 40 °C for 30 min. The mixture was then washed and centrifuged, and the drug carrier (CC) was collected *via* freeze-drying.

CHARACTERIZATION

Microscopy Observations

Transmission electron microscopy (TEM) images of the CNCs, CS, and CC samples were taken using a FEI Tecnai F20 electron microscope (Thermo Fisher Scientific, Waltham, MA, USA) with a 187 kV acceleration voltage. The diluted CNCs, CS, and CC suspensions (0.01 wt.%) were dropped onto the electron microscopy grids with carbon a coating and were subsequently stained with a phosphotungstic acid solution (1 wt.%). Nano Measurer 1.2

(Department of Chemistry, Fudan University, Shanghai, China) was used to calculate the sample diameters from the TEM images.

FTIR Spectroscopy

The Fourier-transform infrared (FTIR) spectra were recorded using a Thermo Nicolet Avatar 360 (Thermo Fisher Scientific, Beijing, China) in the 400 cm^{-1} to 4000 cm^{-1} range.

Thermal Stability

A thermogravimetric analysis was performed using a thermogravimetric analyzer (Pyris 6, Perkin-Elmer, USA) in the 25 °C to 600 °C temperature range and at a heating rate of 10 °C min^{-1} under a constant nitrogen flow.

HES Loading

The CC (50 mg) was fully dispersed in double distilled water (80 mL) *via* ultrasonication, and 2 mL of the HES/methanol solution (0.2 mg mL^{-1}) was added drop by drop to the CC solution under vigorous stirring. The suspension was then incubated at 40 °C under constant stirring for 60 min and centrifuged using a high-speed centrifuge (CT14D, Techcomp Ltd) at 12000 rpm for 15 min. The amount of unbound HES in the supernatant was determined using an ultraviolet–visible (UV/vis) spectrophotometer (TU-1950, Beijing Purkinje General Instruments Co., Ltd, Beijing, China) at 285 nm (Shamloo *et al*. 2015). The flocculent precipitates were collected *via* freeze-drying and labeled CC@HES.

The HES loading capacity (q, mg g^{-1}) was calculated as follows,

$$q = V \times (C_0 - C_e)/m \quad (1)$$

where C_0 and C_e (mg mL^{-1}) are the initial and equilibrium concentrations of the HES in solution, respectively, m is the CC weight (mg), and V is the solution volume (mL).

In Vitro Drug Release

The *in vitro* release profile of CC@HES was studied in a sustained manner, with the physiological condition mimicked using a phosphate-buffered saline (PBS) with pH values of 6.4 and 7.4 at 37 °C.

The suspension was centrifuged at a high speed for less than 1 min at predetermined times, with the supernatant removed for drug quantification *via* UV/vis for HES, as described in "HES loading". A fresh release medium was added to the test tube at each sampling time point, and the drug delivery system was resuspended.

The accumulative percentage release (Q %) was expressed as follows,

$$Q\% = 100 \times (C_n \times V_0 + V_i \sum_{i=1}^{n-1} C_i) / m \quad (2)$$

where C_n (mg mL^{-1}) is the concentration of the drug in the sample, V_0 (mL) is the volume of the release medium, V_i (mL) is the volume of the placed medium, and m (mg) is the amount of drug in the sample.

RESULTS AND DISCUSSION

Microstructures

The TEM images of the CNCs, CS, and CC samples are shown in Fig. 2. It was clear that the CNCs particles showed irregular agglomeration shape, whereas the obtained CS samples

exhibited visibly nearly spherical morphology with diameters of 150 nm to 200 nm. The CC diameters (CS coated with CTMAB) were approximately 250 nm to 290 nm and showed relatively good dispersions compared with the CNCs samples.

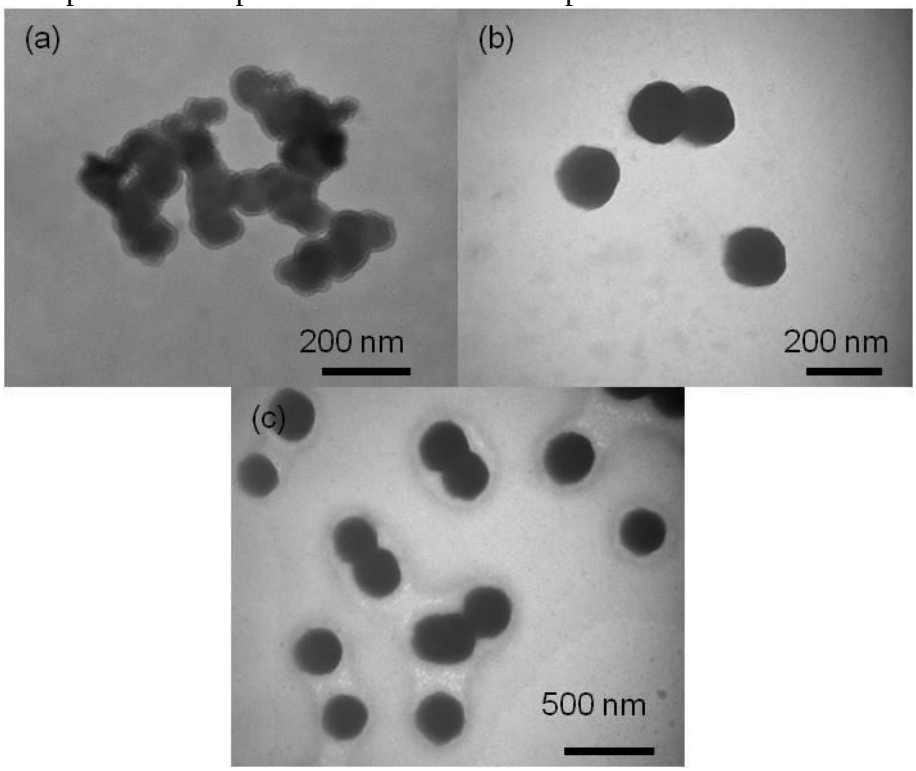

Fig. 2. Micro-morphology of (a) CNCs, (b) CS, and (c) CC

FTIR Analysis

The FTIR spectra were utilized to examine the evolution of the samples during the modification process. The CCs and their intermediate products were evaluated: (a) raw material (RW), (b) CNCs, (c) CS, and (d) CC, which are presented in Fig. 3. The peak at 1509 cm^{-1} in the RW spectrum, which was attributed to the C=C stretching vibration in the aromatic ring of lignin, disappeared completely in the CNCs samples. This indicated that lignin was well removed from the RW after thorough mixing with the aqueous chlorite/acetate buffer solution (Chen *et al*. 2011). The absence of the peak at 1737 cm^{-1} in the CNCs spectrum was attributed to the removal of most of the hemicelluloses during the NaOH treatment (Chen *et al*. 2011). An intensive and broad peak at 3347 cm^{-1} was observed after sulfuric acid hydrolysis and ultrasonication, which was related to the hydrogen-bonded O–H stretching vibration, whereas the peaks at 2925 cm^{-1} and 2850 cm^{-1} were attributed to the stretching vibrations in $–CH_2$ and $–CH_3$, respectively (Shang *et al*. 2016). The peak at 1640 cm^{-1} resulted from O–H bending due to the presence of moisture in the CNCs (Maiti *et al*. 2013). The bands at 1431 cm^{-1} and 897 cm^{-1} were characteristic of the $–CH_2$ bending and C_1–H deformation vibration of cellulose, respectively, whereas the peak at 1059 cm^{-1} was related to the stretching vibration of C–O (Luzi *et al*. 2019). These observations indicated that a large amount of lignin and hemicelluloses were removed during the chemical procedures, with the fabricated CNCs samples exhibiting chemical structures that were typical of cellulose.

A novel peak was observed at 1730 cm^{-1} after SAA grafting, which was attributed to the C=O stretching vibration of the carbonyl group. This observation suggested that the CS was successfully fabricated by grafting SAA onto the CNCs (Stephen *et al*. 2011). No difference

between the spectra of the CS and CC samples after CS modification with CTMAB could be observed, which demonstrated that CTMAB absorption did not change the chemical structure of CS, but rather the CTMAB coating adhering to the CS samples by mere electrostatic interactions.

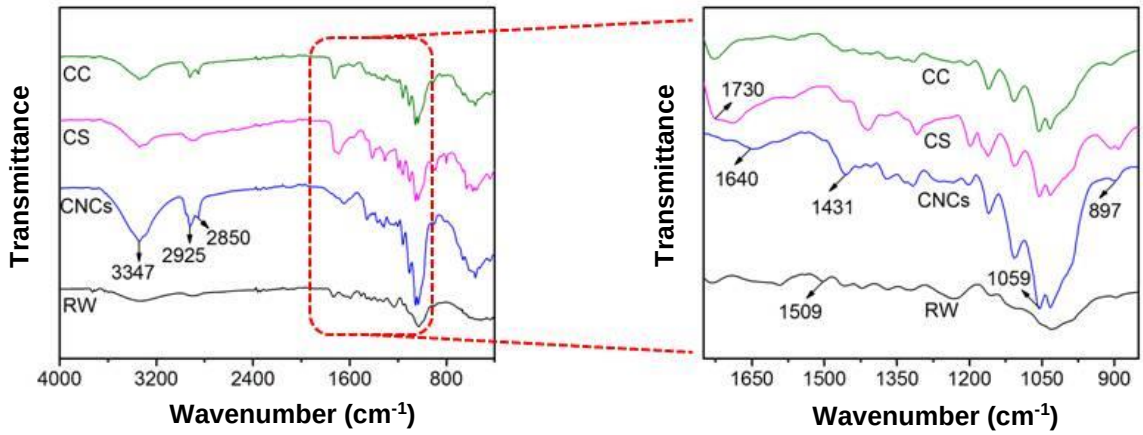

Fig. 3. FTIR spectra of RW, CNCs, CS, and CC

Thermal Properties

The thermogravimetric (TG) and differential thermogravimetric (DTG) curves of RW, CNCs, CS, and CC are shown in Fig. 4. All of the TG curves exhibited a small degree of weight loss between room temperature and 105 °C, which corresponded to moisture loss from all of the sample surfaces (Kasiri and Fathi 2018). The thermal degradation of each of the samples could clearly be divided into two stages. The first stage of RW degradation occurred between 213.8 °C and 341.3 °C, resulting in a weight loss of 53.5 wt% due to the degradation of hemicelluloses, lignin, and pectin (Chen *et al*. 2011). With this observance, the peak around 328.5 °C was attributed to the decomposition of cellulose and lignin (Collazo-Bigliardi *et al*. 2018). The second stage of RW degradation occurred between 380.9 °C and 468.1 °C (peak at 447.5 °C), resulting in a weight loss of 20.57 wt%, due to the ash and lignin.

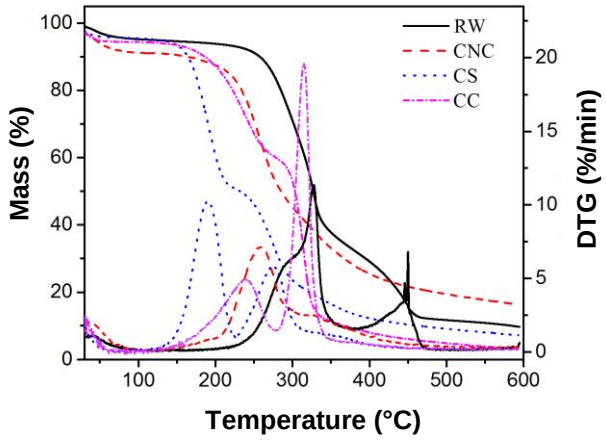

Fig. 4. TG and DTG curves of RW, CNC, CS, and CC

The thermal stability of the CNCs was clearly weaker than that of the RW, which corresponded to the introduction of sulfate groups *via* the sulfuric acid treatment that took place (Jonoobi *et al*. 2015). The onset degradation temperatures of the CS and CC samples during the first degradation stage were 128.9 °C and 129.8 °C, respectively, which might be due to the

grafting of SAA onto the CNCs. The peak degradation temperature of the CC during the first stage (273.7 °C) was higher than that of the CC during the second stage (315.21 °C), which may be due to the CTMAB coating. Compared to CNCs, the thermal stability of the CS and CC samples decreased after modification, which will be improved in future research.

HES Loading

It has been demonstrated that a hydrophobic domain can be fabricated on the CS surface *via* CTMAB coating, and hydrophobic drugs, such as HES, can be strongly partitioned to the CTMAB domains on CS using drug-free solutions at low concentrations (Qing *et al*. 2016). The HES standard curve was determined *via* UV/vis at 285 nm, and the HES load was calculated according to Eq. (1), which yielded an HES load of 37.79 ± 0.6 mg g^{-1} (HES/CC).

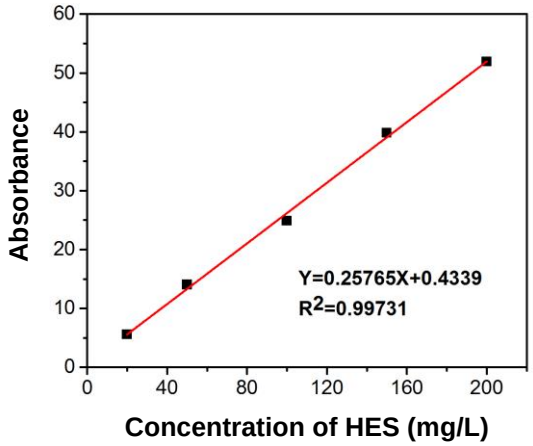

Fig. 5. HES standard curve

Release of the Drug Delivery System

The drug content was analyzed using UV/vis spectrometry at 285 nm, and the assay method was validated. The CC@HES release profiles using PBS solutions at different pH values are shown in Fig. 6, with the HES complex release at a pH of 7.4 generally being higher than the HES complex delivery at pH 6.4. The cumulative drug release from CC@HES was sustained over a 24 h period, indicating a considerable increase in the controlled release time. Only 62 wt% of the HES was released at a pH of 6.4, whereas 71 wt% of the HES was released at a pH of 7.4, which demonstrated that the weak acid drug could easily be ionized under weak alkaline conditions.

The drug delivery vehicle primarily releases drugs through diffusion, swelling, dissolution, permeation, or other mechanisms (Arifin *et al*. 2006; Zhang and Gu 2009). The drug delivery system fabricated here was insoluble in water, which indicated that the degradation of CC@HES was very slow at room temperature in water. Therefore, the drug release from the CC@HES drug delivery vehicle was primarily sustained and controlled *via* diffusion and substrate swelling (Lucht and Peppas 1987; Colombo *et al*. 1996; Arifin *et al*. 2006). The Peppas empirical equation is always used when describing the pharmacokinetics of controlled drug release from a drug delivery vehicle as follows (Lucht and Peppas 1987; Colombo *et al*. 1996; Nappini *et al*. 2011),

$$M_t/M_0 = kt^n \quad (3)$$

where M_t/M_0 is the cumulative drug release (wt%); t is the cumulative release time; k is a constant that depends on both the structural characteristics of the material, as well as, the solvent

and material interactions; *n* is an exponent that is determined by the drug release mechanism and is related to the geometry of the drug delivery vehicle, which is always used as a basis for analyzing the drug release mechanism. Numerous studies (Lucht and Peppas 1987; Colombo *et al*. 1996; Arifin *et al*. 2006) have shown that the *n* values of spherical, cylindrical, and planar systems released *via* a Fickian diffusion mechanism are 0.43, 0.45, and 0.5, respectively, whereas those of the Case II transport mechanism are 0.85, 0.89, and 1.0, respectively. Furthermore, *n* values between 0.43 and 0.85 indicate that anomalous transport has occurred.

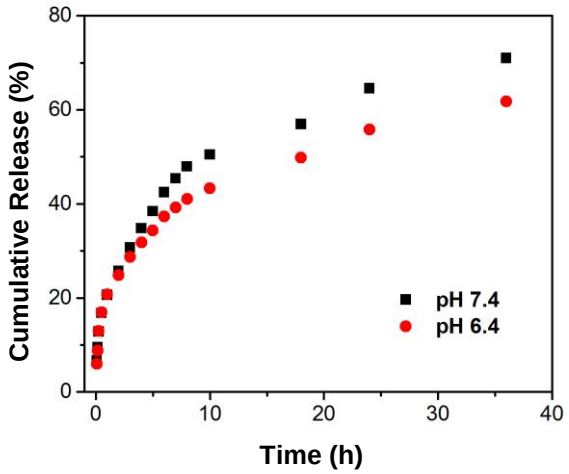

Fig. 6. CC@HES release curves at 37 °C using PBS solutions with different pH values

The applicability of the Peppas empirical equation to the prepared drug delivery vehicle was investigated by transforming Eq. 3 into Eq. 4,

$$log(M_t/M_{t0}) = n\,log(t) + log(k) \quad (4)$$

where M_t/M_0 is the cumulative drug release (wt.%); t is the cumulative release time; k is a constant that depends on both the structural characteristics of the material, as well as, the solvent and material interactions; and n is an exponent that is determined by the drug release mechanism and is related to the geometry of the drug delivery vehicle. The drug release exhibits a strong correlation to the Peppas empirical equation when the cumulative drug release is logarithmic in time and can be linearly correlated. The slope of the best-fit line yields the release exponent, *n*, which can then be used to determine the drug release mechanism.

Table 1. Parameters Obtained from Peppas Equations for HES Release from CC@HES using PBS Solutions with Different pH Values

pH	*n*	*k*	R^2
7.4	0.3609	4.0917	0.9823
6.4	0.3863	20.0207	0.9887

Here, the logarithmic cumulative release exhibited a good linear relationship with time (Fig. 7), which demonstrated that the HES release from CC@HES corresponded well to the Peppas empirical equation ($R^2 \approx 1$), with the fitting results shown in Table 1. The drug diffusion indices (*n*) in the PBS solutions with pH values of 6.4 and 7.4 were both close to 0.43, which specified that the HES release from CC@HES exhibited a Fickian diffusion mechanism (Namazi and Kanani 2009). Diffusion was therefore the key factor for HES release from CC@HES.

However, the HES release was slightly different from the spherical, cylindrical, and planar system releases *via* the Fickian diffusion. This may be related to the micro-morphology of CC (nonstandard spheres), which is shown in the CC TEM image (Fig. 2. c).

All these results demonstrated that prepared CC samples could be utilized as drug delivery carriers and the release of HES from CC@HES has higher efficiency and rate at a pH of 7.4, which may be caused by phenolic hydroxyl groups on HES (Tripoli *et al*. 2007).

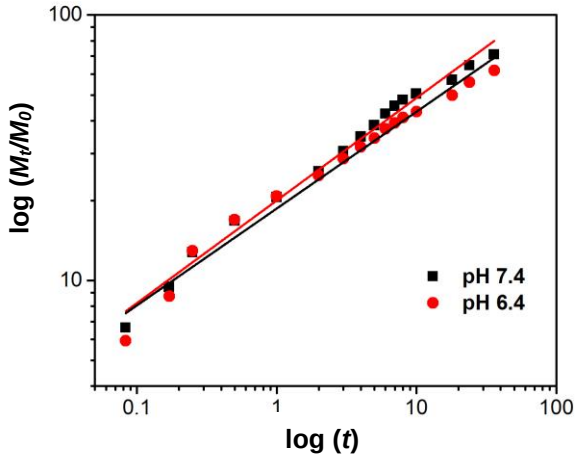

Fig. 7. The HES release curves from CC@HES based on the Peppas equation in Eq. (4), with the straight lines representing the best-fit lines of the data

CONCLUSIONS

1. Cellulose nanocrystals (CNCs) were synthesized from rubber wood (RW). The CNCs were then modified with succinic anhydride (SAA) and coated with cetyltrimethyl ammonium bromide (CTMAB) to prepare the drug carrier, CC. TEM images showed that the CS and CC samples were torispherical. Furthermore, the CC samples presented relatively good dispersions in comparison to the CNCs samples.
2. FTIR analysis indicated that SAA was successfully grafted onto the CNCs, and the CS samples were coated with CTMAB by mere electrostatic interactions.
3. The drug release curves demonstrated that the HES complex release at a pH of 7.4 (71 wt.%) was higher than the HES complex delivery at a pH of 6.4 (62 wt.%), which indicated that the weak acid drug could be easily ionized under weak alkaline conditions.
4. The logarithmic cumulative release exhibited a good linear relationship with time. Additionally, the drug diffusion indices (*n*) in PBS solutions with pH values of 6.4 and 7.4 were close to 0.43, which indicated that the HES release from CC@HES corresponded well to the Peppas empirical equation and exhibited a Fickian diffusion mechanism.
5. A novel hydrophobic drug delivery vehicle with spherical shape was established based on the CNCs fabricated from RW and could offer a mechanism for the high-value application of RW.

ACKNOWLEDGMENTS

The authors express their appreciation to Key Laboratory of Bio-based Material Science and Technology of Ministry of Education and College of Material Science and Engineering of Northeast Forestry University for full support of this research.

REFERENCES CITED

Arifin, D. Y., Lee, L. Y., and Wang, C. H. (2006). "Mathematical modeling and simulation of drug release from microspheres: Implications to drug delivery systems," *Advanced Drug Delivery Reviews* 58(12-13), 1274-1325. DOI: 10.1016/j.addr.2006.09.007

Beck-Candanedo, S., Roman, M., and Gray, D. G. (2005). "Effect of reaction conditions on the properties and behavior of wood cellulose nanocrystal suspensions," *Biomacromolecules* 6(2), 1048-1054. DOI: 10.1021/bm049300p

Boluk, Y., Lahiji, R., Zhao, L. Y., and McDermott, M. T. (2011). "Suspension viscosities and shape parameter of cellulose nanocrystals (CNC)," *Colloids and Surfaces a-Physicochemical and Engineering Aspects* 377(1-3), 297-303. DOI: 10.1016/j.colsurfa.2011.01.003

Brito, B. S. L., Pereira, F. V., Putaux, J. L., and Jean, B. (2012). "Preparation, morphology and structure of cellulose nanocrystals from bamboo fibers," *Cellulose* 19(5), 1527-1536. DOI: 10.1007/s10570-012-9738-9

Camargo, L. A., Pereira, S. C., Correa, A. C., Farinas, C. S., Marconcini, J. M., and Mattoso, L. H. C. (2016). "Feasibility of manufacturing cellulose nanocrystals from the solid residues of second-generation ethanol production from sugarcane bagasse," *Bioenergy Research* 9(3), 894-906. DOI: 10.1007/s12155-016-9744-0

Chen, W., Yu, H., and Liu, Y. (2011). "Preparation of millimeter-long cellulose I nanofibers with diameters of 30-80 nm from bamboo fibers," *Carbohydrate Polymers* 86(2), 453-461. DOI: 10.1016/j.carbpol.2011.04.061

Collazo-Bigliardi, S., Ortega-Toro, R., and Chiralt Boix, A. (2018). "Isolation and characterisation of microcrystalline cellulose and cellulose nanocrystals from coffee husk and comparative study with rice husk," *Carbohydrate Polymers* 191, 205-215. DOI: 10.1016/j.carbpol.2018.03.022

Colombo, P., Bettini, R., Santi, P., De Ascentiis, A., and Peppas, N. A. (1996). "Analysis of the swelling and release mechanisms from drug delivery systems with emphasis on drug solubility and water transport," *Journal of Controlled Release* 39(2), 231-237. DOI: 10.1016/0168-3659(95)00158-1

de Rodriguez, N. L. G., Thielemans, W., and Dufresne, A. (2006). "Sisal cellulose whiskers reinforced polyvinyl acetate nanocomposites," *Cellulose* 13(3), 261-270. DOI: 10.1007/s10570-005-9039-7

Habibi, Y., Lucia, L. A., and Rojas, O. J. (2010). "Cellulose nanocrystals: Chemistry, self-assembly, and applications," *Chemical Reviews* 110(6), 3479-3500. DOI: 10.1021/cr900339w

Hasan, A., Waibhaw, G., Tiwari, S., Dharmalingam, K., Shukla, I., and Pandey, L. M. (2017). "Fabrication and characterization of Chitosan, polyvinylpyrrolidone and cellulose nanowhiskers nanocomposite films for wound healing drug delivery application," *Journal of Biomedical Materials Research Part A* 105(A), 2391-2404. DOI: 10.1002/jbm.a.36097

Hasan, A., Waibhaw, G., Saxena, V., and Pandey, L. M. (2018). "Nano-biocomposite scaffolds of chitosan, carboxymethyl cellulose and silver nanoparticle modified cellulose nanowhiskers

for bone tissue engineering applications," *International Journal of Biological Macromolecules* 111, 923-934. DOI: 10.1016/j.ijbiomac.2018.01.089

Huang, Y. (2008). "World rubber wood production and sales and its development prospects," *China Tropical Agriculture* 6, 25-28. (in Chinese)

Jonoobi, M., Oladi, R., Davoudpour, Y., Oksman, K., Dufresne, A., Hamzeh, Y., and Davoodi, R. (2015). "Different preparation methods and properties of nanostructured cellulose from various natural resources and residues: a review," *Cellulose* 22(2), 935-969. DOI: 10.1007/s10570-015-0551-0

Kasiri, N., and Fathi, M. (2018). "Production of cellulose nanocrystals from pistachio shells and their application for stabilizing Pickering emulsions," *International Journal of Biological Macromolecules* 106, 1023-1031. DOI: 10.1016/j.ijbiomac.2017.08.112

Kontturi, E., Laaksonen, P., Linder, M. B., Nonappa, Groechel, A. H., Rojas, O. J., and Ikkala, O. (2018). "Advanced materials through assembly of nanocelluloses," *Advanced Materials* 30(24), 1703779. DOI: 10.1002/adma.201703779

Li, X., Li, M., Qin, S., Jiang, J., Lu, Q., and Li, J. (2016). "Effect of steam pressure on physical and mechanical properties of thermally modified rubber wood," *Chinese Journal of Tropical Agriculture* 36(11), 106-110. DOI: 10.12008/j.issn.1009-2196.2016.11.022 (in Chinese)

Lucht, L. M., and Peppas, N. A. (1987). "Transport of penetrants in the macromolecular structure of coals. V. Anomalous transport in pretreated coal particles," *Journal of Applied Polymer Science* 33(5), 1557-1566. DOI: 10.1002/app.1987.070330511

Luzi, F., Puglia, D., Sarasini, F., Tirillo, J., Maffei, G., Zuorro, A., Lavecchia, R., Kenny, J. M., and Torre, L. (2019). "Valorization and extraction of cellulose nanocrystals from North African grass: *Ampelodesmos mauritanicus (Diss)*," *Carbohydrate Polymers* 209, 328-337. DOI: 10.1016/j.carbpol.2019.01.048

Maiti, S., Jayaramudu, J., Das, K., Reddy, S. M., Sadiku, R., Ray, S. S., and Liu, D. (2013). "Preparation and characterization of nano-cellulose with new shape from different precursor," *Carbohydrate Polymers* 98(1), 562-567. DOI: 10.1016/j.carbpol.2013.06.029

Mondragon, G., Santamaria-Echart, A., Hormaiztegui, M. E. V., Arbelaiz, A., Pena-Rodriguez, C., Mucci, V., Corcuera, M., Aranguren, M. I., and Eceiza, A. (2018). "Nanocomposites of waterborne polyurethane reinforced with cellulose nanocrystals from sisal fibres," *Journal of Polymers and the Environment* 26(5), 1869-1880. DOI: 10.1007/s10924-017-1089-z

Namazi, H., and Kanani, A. (2009). "Investigation diffusion mechanism of beta-lactam conjugated telechelic polymers of PEG and beta-cyclodextrin as the new nanosized drug carrier devices," *Carbohydrate Polymers* 76(1), 46-50. DOI: 10.1016/j.carbpol.2008.09.023

Nappini, S., Bonini, M., Bombelli, F. B., Pineider, F., Sangregorio, C., Baglioni, P., and Norden, B. (2011). "Controlled drug release under a low frequency magnetic field: Effect of the citrate coating on magnetoliposomes stability," *Soft Matter* 7(3), 1025-1037. DOI: 10.1039/c0sm00789g

Nielsen, I. L. F., Chee, W. S. S., Poulsen, L., Offord-Cavin, E., Rasmussen, S. E., Frederiksen, H., Euslen, M., Barron, D., Horcajada, M. N., and Williamson, G. (2006). "Bioavailability is improved by enzymatic modification of the citrus flavonoid hesperidin in humans: A randomized, double-blind, crossover trial1," *The Journal of Nutrition* 136(2), 404-408. DOI: 10.1093/jn/136.2.404

Qin, S., Li, X., Li, M., and Li, X. (2017). "Present situation, prospect and suggestion of Chinese rubber wood modification technology," *Tropical Agricultural Engineering* 41(4), 69-72. (in Chinese)

Qing, W., Wang, Y., Wang, Y., Zhao, D., Liu, X., and Zhu, J. (2016). "The modified nanocrystalline cellulose for hydrophobic drug delivery," *Applied Surface Science* 366(#), 404-409. DOI: 10.1016/j.apsusc.2016.01.133

Rao, K. M., Kumar, A., and Han, S. S. (2017). "Polysaccharide based bionanocomposite hydrogels reinforced with cellulose nanocrystals: Drug release and biocompatibility analyses," *International Journal of Biological Macromolecules* 101, 165-171. DOI: 10.1016/j.ijbiomac.2017.03.080

Sacui, I. A., Nieuwendaal, R. C., Burnett, D. J., Stranick, S. J., Jorfi, M., Weder, C., Foster, E. J., Olsson, R. T., and Gilman, J. W. (2014). "Comparison of the properties of cellulose nanocrystals and cellulose nanofibrils isolated from bacteria, tunicate, and wood processed using acid, enzymatic, mechanical, and oxidative methods," *ACS Applied Materials & Interfaces* 6(9), 6127-6138. DOI: 10.1021/am500359f

Sehaqui, H., Kulasinski, K., Pfenninger, N., Zimmermann, T., and Tingaut, P. (2017). "Highly carboxylated cellulose nanofibers *via* succinic anhydride esterification of wheat fibers and facile mechanical disintegration," *Biomacromolecules* 18(1), 242-248. DOI: 10.1021/acs.biomac.6b01548

Shamloo, M. M., Sharifani, M., Garmakhany, A. D., and Seifi, E. (2015). "Alternation of secondary metabolites and quality attributes in Valencia Orange fruit (*Citrus sinensis*) as influenced by storage period and edible covers," *Journal of Food Science and Technology-Mysore* 52(4), 1936-1947. DOI: 10.1007/s13197-013-1207-4

Shang, W., Sheng, Z., Shen, Y., Ai, B., Zheng, L., Yang, J., and Xu, Z. (2016). "Study on oil absorbency of succinic anhydride modified banana cellulose in ionic liquid," *Carbohydrate Polymers* 141, 135-142. DOI: 10.1016/j.carbpol.2016.01.009

Stephen, M., Catherine, N., Brenda, M., Andrew, K., Leslie, P., and Corrine, G. (2011). "Oxolane-2,5-dione modified electrospun cellulose nanofibers for heavy metals adsorption," *Journal of Hazardous Materials* 192(2), 922-927. DOI: 10.1016/j.jhazmat.2011.06.001

Tripoli, E., Guardia, M. L., Giammanco, S., Majo, D. D., and Giammanco, M. (2007). "Citrus flavonoids: molecular structure, biological activity and nutritional properties: A review," *Food Chemistry* 104(2), 466-479. DOI: 10.1016/j.foodchem.2006.11.054

Wu, Q. F., Liu, W. B., Zhuo, C. X., Rong, Z. Q., Ye, K. Y., and You, S. L. (2011). "Iridium-catalyzed intramolecular asymmetric allylic dearomatization of phenols," *Angewandte Chemie-International Edition* 50(19), 4455-4458. DOI: 10.1002/anie.201100206

Zhang, J., and Gu, J. (2009). "Dynamics of controlled/sustained release dosage form," *Science Press* Beijing, pp. 27-50. (in Chinese)

Zheng, D., Li, M., Zhang, X., and Yue, J. (2019). "Preparation of cellulose nanofibrils from rubber wood," *Packaging Engineering* 40(3), 100-107. DOI: 10.19554/j.cnki.1001-3563.2019.03.014 (in Chinese)

Article submitted: June 6, 2019; Peer review completed: July 14, 2019; Revised version received: August 5, 2019; Accepted: August 7, 2019; Published: August 9, 2019.
DOI: 10.15376/biores.14.4.7763-7774